

Determination of the Active Site Protonation State of β -Secretase from Molecular Dynamics Simulation and Docking Experiment: Implications for Structure-Based Inhibitor Design

Hwangseo Park* and Sangyoub Lee*

Contribution from the School of Chemistry and Molecular Engineering, and Center for Molecular Catalysis, Seoul National University, Seoul 151-747, South Korea

Received July 23, 2003; E-mail: hwangseo@snu.ac.kr; sangyoub@snu.ac.kr

Abstract: Memapsin 2 (BACE) is an aspartyl protease known as β -secretase that acts on the production of the β -amyloid peptide in the human brain, a key event in the pathogenesis of Alzheimer's disease. Although it is expected that the net charge of the catalytic Asp diad would be -1 as in other kinds of aspartyl proteases, the exact protonation states of Asp32 and Asp228 have not been known without ambiguity. Two independent molecular dynamics (MD) simulations of BACE in complex with the potent inhibitor OM99-2 are carried out to determine the preferred protonation state of the Asp diad in the context that is consistent with the previous X-ray crystal structure. The results show that a strong hydrogen bond between the inhibitor hydroxyl group and Asp228 can be maintained only when Asp32 is neutral and Asp228 is ionized. The preference of this protonation state is further supported from the energetic and structural features found in the docking experiment of a novel potent inhibitor with the BACE active site. Thus, both MD and docking studies suggest that the role of hydrogen bond acceptor for the hydroxyl and piperazine groups of the inhibitors should be played by Asp228 instead of Asp32. This may be a key piece of information for the structure-based design/discovery of new inhibitor drugs.

Introduction

It is well established that the Alzheimer's disease (AD) stems from the accumulation of 40/42-residue amyloid β -peptide ($A\beta$), leading to the formation of insoluble plaques in the brain.¹ A key step in the production of $A\beta$ is the cleavage of a membrane protein called the amyloid precursor protein (APP) by a protease known as β -secretase (BACE), which has been identified as a membrane-anchored aspartic protease termed memapsin 2.² Therefore, the in vivo inhibition of BACE is likely to reduce the production of $A\beta$ and thereby delay or halt the progression of AD. Therefore, the discovery of inhibitor drugs for β -secretase has been regarded as the major therapeutic strategy for the treatment of AD.

Most of the BACE inhibitors identified so far are peptidomimetic transition state analogues, and involve a hydroxyethyl group targeted to be hydrogen-bonded to the Asp32-Asp228 catalytic diad by displacing a catalytic water molecule.³ Despite their high inhibitory strengths, however, such mechanism-based compounds are unlikely to be good drug candidates because of their high molecular weights and their poor ability to pass through the biological membrane.⁴ Nonetheless, the determination of X-ray crystal structures of BACE in complex with the potent inhibitors, such as OM99-2 and OM00-3 (Figure 1), is likely to accelerate the discovery of a new inhibitor drug through the various structure-based approaches including virtual screening and de novo design methods.^{3b,3c}

It is generally agreed that in the catalytic hydrolysis of a peptide by aspartic proteases such as pepsin, penicillopepsin, rennin, and HIV-1 protease, two active-site aspartyl residues operate cooperatively with net charge of -1 .⁵ Because BACE has a pH rate profile similar to HIV-1 protease,⁶ its two catalytic residues (Asp32 and Asp228) are also believed to participate

(1) (a) Hardy, J.; Selkoe, D. J. *Science* **2002**, *297*, 353–356, and references therein. (b) Strooper, B. D.; Knig, G. *Nature* **1999**, *402*, 471–472.

(2) (a) Vassar, R.; Bennett, B. D.; Babu-Khan, S.; Kahn, S.; Mendiaz, E. A.; Denis, P.; Teplow, D. B.; Ross, S.; Amarante, P.; Loeloff, R.; Luo, Y.; Fisher, S.; Fuller, J.; Edenson, S.; Lile, J.; Jarosinski, M. A.; Biere, A. L.; Curran, E.; Burgess, T.; Louis, J. C.; Collins, F.; Treanor, J.; Rogers, G.; Citron, M. *Science* **1999**, *286*, 735–741. (b) Sinha, S.; Anderson, J. P.; Barbour, R.; Basi, G. S.; Caccavello, R.; Davis, D.; Doan, M.; Dovey, H. F.; Frigon, N.; Hong, J.; Jacobson-Croak, K.; Jewett, N.; Keim, P.; Knops, J.; Lieberburg, I.; Power, M.; Tan, H.; Tatsuno, G.; Tung, J.; Schenk, D.; Seubert, P.; Suomensaaari, S. M.; Wang, S.; Walker, D.; John, V. *Nature* **1999**, *402*, 537–540. (c) Yan, R.; Bienkowsky, M. J.; Shuck, M. E.; Miao, H.; Tory, M. C.; Pauley, A. M.; Brashier, J. R.; Stratman, N. C.; Mathews, W. R.; Buhl, A. E.; Carter, D. B.; Tomasselli, A. G.; Parodi, L. A.; Heinrichson, R. L.; Gurney, M. E. *Nature* **1999**, *402*, 533–537. (d) Hussain, I.; Powell, D.; Howlett, D. R.; Tew, D. G.; Meek, T. D.; Chapman, C.; Gloger, I. S.; Murphy, K. E.; Southan, C. D.; Ryan, D. M.; Smith, T. S.; Simmons, D. L.; Walsh, F. S.; Dingwall, C.; Christie, G. *Mol. Cell. Neurosci.* **1999**, *14*, 419–427. (e) Lin, X.; Koelsch, G.; Wu, S.; Downs, D.; Dashti, A.; Tang, J. *Proc. Natl. Acad. Sci. U.S.A.* **2000**, *97*, 1456–1460.

(3) (a) Ghosh, A. K.; Shin, D.; Downs, D.; Koelsch, G.; Tang, J. *J. Am. Chem. Soc.* **2000**, *122*, 3522–3523. (b) Hong, L.; Koelsch, G.; Lin, X.; Wu, S.; Terzian, S.; Ghosh, A. K.; Zhang, X. C.; Tang, J. *Science* **2000**, *290*, 150–153. (c) Ghosh, A. K.; Bilcer, G.; Harwood, C.; Kawahama, R.; Shin, D.; Hussain, K. A.; Hong, L.; Loy, J. A.; Nguyen, C.; Koelsch, G.; Ermolieff, J.; Tang, J. *J. Med. Chem.* **2001**, *44*, 2865–2868. (d) Tung, J. S.; Davis, D. L.; Anderson, J. P.; Walker, D. E.; Mamo, S.; Jewett, N.; Hom, R. K.; Sinha, S.; Thorsett, E. D.; John, V. *J. Med. Chem.* **2002**, *45*, 259–262. (e) Hong, L.; Turner, R. T.; Koelsch, G.; Shin, D.; Ghosh, A. K.; Tang, J. *Biochemistry* **2002**, *41*, 10 963–10 967.

(4) Wolfe, M. S. *Nature Rev. Drug Discov.* **2002**, *1*, 859–866.

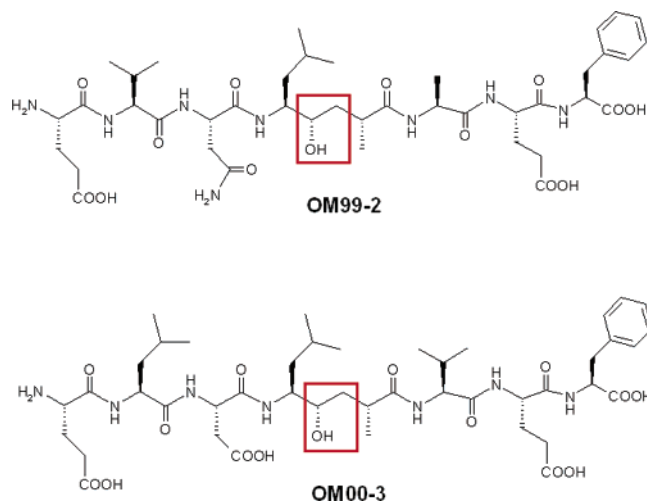


Figure 1. Molecular structures of OM99-2 and OM00-3. Indicated with red box is the hydroxyethyl group mimicking the transition state for hydrolysis of a peptide bond.

in substrate binding and enzymatic reaction in their opposite protonation states. However, it has not been possible to determine the exact protonation state of each catalytic residue in an unambiguous manner.⁷ Because the protonation state of active site residues may have a significant effect on the results of the structure-based virtual screening processes,⁸ the correct assignment of the protonation states of Asp32 and Asp228 is essential for the efficient discovery of a new potent BACE inhibitor.

The ambiguity of the protonation states of Asp32 and Asp228 stems from the lack of their proton coordinates in the X-ray crystal structures of BACE in complex with OM99-2 and OM00-3. As mentioned above, both inhibitors are eight-residue peptidomimetic, having a hydroxyethyl group as a mimic of the transition state for peptide hydrolysis. On the basis of the interatomic distances between the hydroxyl oxygen of the inhibitor and the carboxylate oxygens of catalytic Asp residues in the original X-ray crystal structure, two possibilities for the hydrogen-bonding patterns may be proposed differing in the protonation state of the Asp diad with the net charge of -1 . The first (Model I in Figure 2) involves the neutral Asp32 and deprotonated Asp228, with the inhibitor hydroxyl group playing the roles of hydrogen bond donor and hydrogen bond acceptor with respect to Asp228 and Asp32, respectively. The protonation states of the two Asp residues are reversed in the other possibility (Model II in Figure 2), in which the inhibitor hydroxyl moiety receives a hydrogen bond from Asp228 and donates a hydrogen bond to Asp32.

In the present study, we try to determine the preferred protonation state of the catalytic Asp diad by comparing stabilities of the two hydrogen bond patterns illustrated in Figure

2 using the solution-phase molecular dynamics (MD) simulations. On the basis of docking experiment of the novel potent inhibitor, WO02088101 (see Figure 3),⁹ in the two different forms of BACE, it will be addressed that the precise assignment of protonation state of the catalytic Asp diad should be a prerequisite for the structure-based virtual screening of new BACE inhibitors.

Computational Methods

Molecular Dynamics Simulation. MD simulations of the BACE in complex with OM99-2 were carried out using the SANDER module of AMBER⁷¹⁰ with the force field reported by Cornell et al.¹¹ Using the X-ray crystal structure of BACE-OM99-2 complex,^{3b} the two starting coordinates were prepared in such a way that the protonation states of Asp32 and Asp228 should be opposite. The geometry of OM99-2 was fully optimized at RHF/6-31G* level of theory with the *Gaussian 98* suite¹² to compute the electrostatically derived atomic charges¹³ through the RESP method.¹⁴ Missing force field parameters for OM99-2 were estimated from similar chemical species in the AMBER database.

The all-atom models for the BACE-OM99-2 complex was neutralized by adding sodium ions and then was immersed in a rectangular box containing 12 763 TIP3P water molecules.¹⁵ After 1000 cycles of energy minimization to remove the bad van der Waals contacts, we equilibrated both systems, beginning with 20 ps equilibration dynamics of the solvent molecules at 300 K. The next step involved equilibration of the solute with a fixed configuration of the solvent molecules for 5 ps at 10, 50, 100, 150, 200, 250, and 300 K. Then, the equilibration dynamics of the entire system was performed at 300 K for 20 ps. Following the equilibration procedure, 1.2 ns MD simulations were carried out with a periodic boundary condition in the NPT ensemble at 300 K using Berendsen temperature coupling¹⁶ and constant pressure (1 atm) with isotropic molecule-based scaling. The SHAKE algorithm,¹⁷ with a tolerance of 10^{-6} , was applied to fix all bond lengths involving hydrogen atom. We used a time step of 1.5 fs and a nonbond-interaction cutoff radius of 12 Å; the trajectory was sampled every 0.15 ps (100 step intervals) for analyses.

Docking Experiments. The calculations were performed using the software package DOCK 4.0,¹⁸ running on Silicon Graphics OCTANE R10000. First, a Connolly surface¹⁹ of the BACE active site was generated by using a 1.4 Å probe radius, followed by the generation

- (5) (a) Beveridge, A. J.; Heywood, G. C. *Biochemistry* **1993**, *32*, 3325. (b) Beveridge, A. J.; Heywood, G. C. *J. Mol. Struct.* **1994**, *306*, 235. (c) Trylska, J.; Antosiewicz, J.; Geller, M.; Hodge, C. N.; Klabe, R. M.; Head, M. S.; Gilson, M. K. *Protein Sci.* **1999**, *8*, 180. (d) Park, H.; Suh, J.; Lee, S. *J. Am. Chem. Soc.* **2000**, *122*, 3901–3908. (e) Okimoto, N.; Tsukui, T.; Kitayama, K.; Hata, M.; Hoshino, T.; Tsuda, M. *J. Am. Chem. Soc.* **2000**, *122*, 5613–5622.
- (6) (a) Gruninger-Leitch, F.; Schlatter, D.; Kung, E.; Nelbock, P.; Dobeli, H. *J. Biol. Chem.* **2002**, *277*, 4687–4693. (b) Hyland, L. J.; Tomaszek, T. A. J.; Meek, T. D. *Biochemistry* **1991**, *30*, 8454.
- (7) Toung, B. A.; Reynolds, C. H. *J. Med. Chem.* **2003**, *46*, 2074–2082.
- (8) (a) Roche, O.; Kiyama, R.; Brooks, C. L., III. *J. Med. Chem.* **2001**, *44*, 3592–3598. (b) Rastelli, G.; Pacchioni, S.; Sirawaraporn, W.; Sirawaraporn, R.; Parenti, M. D.; Ferrari, A. M. *J. Med. Chem.* **2003**, *46*, 2834–2845.
- (9) Bhisetti, G. R.; Saunders, J. O.; Murcko, M. A.; Lepre, C. A.; Britt, S. D.; Come, J. H.; Deninger, D. D.; Wang, T. Patent WO02088101, 2002.
- (10) Case, D. A.; Pearlman, D. A.; Caldwell, J. W.; Cheatham, T. E., III; Ross, W. S.; Simmerling, C.; Darden, T.; Merz, K. M., Jr.; Stanton, R. V.; Chen, A.; Vincent, J. J.; Crowley, M.; Tsui, V.; Radmer, R.; Duan, Y.; Pitera, J.; Massova, I.; Seibel, G. L.; Singh, U. C.; Weiner, P.; Kollman, P. A. 2002, AMBER 7, University of California, San Francisco.
- (11) Cornell, W. D.; Cieplak, P.; Bayly, C. I.; Gould, I. R.; Merz, K. M., Jr.; Ferguson, D. M.; Spellmeyer, D. C.; Fox, T.; Caldwell, J. W.; Kollman, P. A. *J. Am. Chem. Soc.* **1995**, *117*, 5179–5197.
- (12) Frisch, M. J.; Trucks, G. W.; Schlegel, H. B.; Scuseria, G. E.; Robb, M. A.; Cheeseman, J. R.; Zakrzewski, V. G.; Montgomery, J., J. A.; Stratmann, R. E.; Burant, J. C.; Dapprich, S.; Millam, J. M.; Daniels, A. D.; Kudin, K. N.; Strain, M. C.; Farkas, O.; Tomasi, J.; Barone, V.; Cossi, M.; Cammi, R.; Mennucci, B.; Pomelli, C.; Adamo, C.; Clifford, S.; Ochterski, J.; Petersson, G. A.; Ayala, P. Y.; Cui, Q.; Morokuma, K.; Malick, D. K.; Rabuck, A. D.; Raghavachari, K.; Foresman, J. B.; Cioslowski, J.; Ortiz, J. V.; Stefanov, B. B.; Liu, G.; Liashenko, A.; Piskorz, P.; Komaromi, I.; Gomperts, R.; Martin, R. L.; Fox, D. J.; Keith, T.; Al-Laham, M. A.; Peng, C. Y.; Nanayakkara, A.; Gonzalez, C.; Challacombe, M.; Gill, P. M. W.; Johnson, B.; Chen, W.; Wong, M. W.; Andres, J. L.; Gonzalez, C.; Head-Gordon, M.; Replogle, E. S.; Pople, J. A. *Gaussian 98*, revision A.7, Gaussian, Inc., Pittsburgh, PA, 1998.
- (13) Besler, B. H.; Merz, K. M., Jr.; Kollman, P. A. *J. Comput. Chem.* **1990**, *11*, 431–439.
- (14) Bayly, C. A.; Cieplak, P.; Cornell, W. D.; Kollman, P. A. *J. Phys. Chem.* **1993**, *97*, 10 269–10 280.
- (15) Jorgensen, W. L.; Chandrasekhar, J.; Madura, J. D.; Impey, R. W.; Klein, M. L. *J. Chem. Phys.* **1983**, *79*, 926–935.
- (16) Berendsen, H. C.; Postma, J. P. M.; van Gunsteren, W. F.; DiNola, A.; Haak, J. R. *J. Comput. Phys.* **1984**, *81*, 3684–3690.
- (17) Ryckaert, J. P.; Ciccoliti, G.; Berendsen, H. C. *J. Comput. Phys.* **1977**, *23*, 327–341.

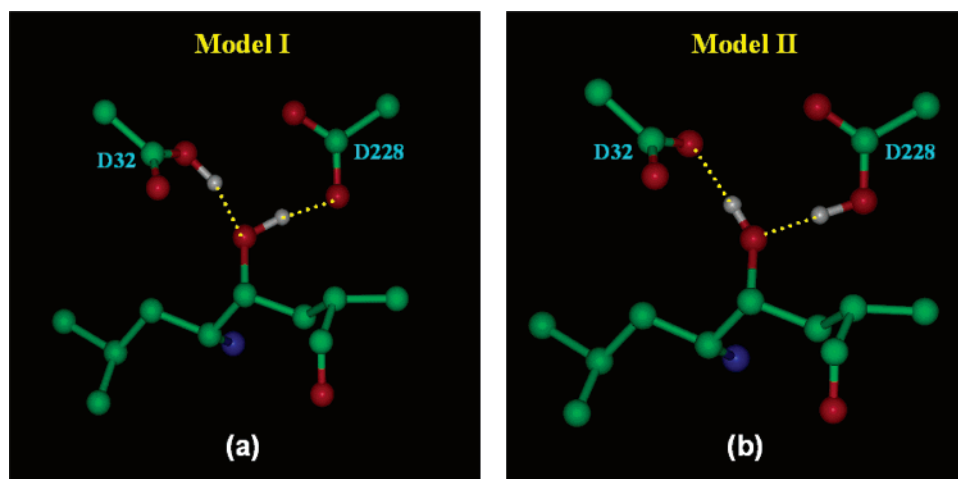


Figure 2. Two possible protonation states of the catalytic Asp residues in the BACE-OM99-2 complex represented by (a) Model I in which Asp32 is neutral and Asp228 is ionized, and (b) Model II with the reversed protonation states. Yellow dotted line indicate hydrogen bonds. The structures are prepared by extracting coordinates of each atom from X-ray crystal structure, followed by adding two hydrogen atoms.

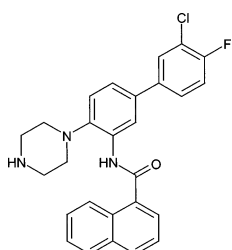


Figure 3. Molecular structure of the novel potent inhibitor WO02088101.

of a set of overlapping spheres that were then clustered according to their spatial distribution. The spheres located too distant from the OM99-2 position were eliminated in the final model cluster. To compute interaction energies, a 3-D grid of 0.3 Å resolution was centered on the OM99-2 position in the X-ray crystal structure. The size of the grid box was chosen to enclose all selected spheres using an extra margin of 6 Å. The grid had a size of about $22 \times 23 \times 22$ Å and was composed of about 11 132 grid points. Energy scoring grids were obtained by using an all-atom model and a distance-dependent dielectric function ($\epsilon = 4r$) with a 10 Å cutoff. Gasteiger–Marsili charges²⁰ were assigned to all protein and ligand atoms. The inhibitor WO02088101 was then docked into the BACE active site by matching sphere centers with the ligand atoms. A flexible docking with subsequent minimization was performed using AMBER force field scoring to generate 200 solutions corresponding to the best energy scores of about a million orientations with varying molecular conformations of the OM99-2. Because binding to the catalytic Asp diad is believed to be necessary in BACE inhibition, only the solutions involving at least one atom within a distance of 5 Å from Asp32 or Asp228 are selected for further analyses.

Results and Discussion

MD Simulation. Shown in Figure 4 are the root-mean-square deviations from X-ray crystal structure ($\text{rmsd}_{\text{x-ray}}$) as a function of simulation time for the two models of the BACE-OM99-2 complex differing in the protonation states of Asp32 and Asp228. The values were obtained by fitting all heavy atoms

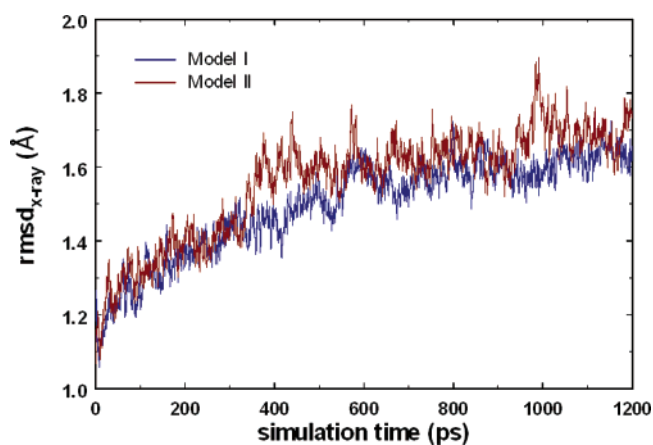


Figure 4. Time dependence of the root-mean-square deviation from the X-ray crystal structure ($\text{rmsd}_{\text{x-ray}}$) for Model I (blue) and Model II (red).

of both BACE and OM99-2 to the crystal structure. The $\text{rmsd}_{\text{x-ray}}$ values remain between 1.06 and 1.73 Å in Model I, with an average of 1.50 Å, and between 1.07 and 1.90 Å in Model II, with an average of 1.56 Å, indicating that neither has revealed a significant structural instability during the entire course of simulation. In addition to the narrower range of $\text{rmsd}_{\text{x-ray}}$, Model I has lower $\text{rmsd}_{\text{x-ray}}$ values than those of Model II for 81% of the simulation time. Thus, the enzyme–inhibitor complex with neutral Asp32 and ionized Asp228 is likely to remain more stable than that with opposite protonation state.

Further evidence for the stability of protein structure in the course of the simulations may be provided by examining the time evolution of rmsd from the starting structure of production dynamics ($\text{rmsd}_{\text{init}}$), which is displayed in Figure 5. The $\text{rmsd}_{\text{init}}$ values of all C α atoms of BACE remain within 1.5 Å for both Model I and Model II with a convergent behavior with respect to the simulation time. Irrespective of the protonation state of the catalytic Asp diad, the $\text{rmsd}_{\text{init}}$ values of ligand are lower than those of BACE C α atoms during the entire course of simulation. This suggests that the movement of OM99-2 should be insignificant within the active site compared to the conformational changes of the protein, which is not surprising for its high potency ($K_i = 1.6$ nM). The insignificant mobility observed

- (18) (a) Meng, E. C.; Shoichet, B. K.; Kuntz, I. D. *J. Comput. Chem.* **1992**, *13*, 505–524. (b) Meng, E. C.; Gschwend, D. A.; Blaney, J. M.; Kuntz, I. D. *Proteins: Struct., Funct., Genet.* **1993**, *17*, 266–278. (c) Shoichet, B. K.; Bodian, D. L.; Kuntz, I. D. *J. Comput. Chem.* **1992**, *13*, 380–397. (d) Ewing, T. J. A.; Kuntz, I. D. *J. Comput. Chem.* **1997**, *18*, 1175–1189.
- (19) Connolly, M. L. The molecular surface package. *J. Mol. Graphics* **1993**, *11*, 139–141.
- (20) Gasteiger, J.; Marsili, M. *Tetrahedron* **1980**, *36*, 3219–3228.

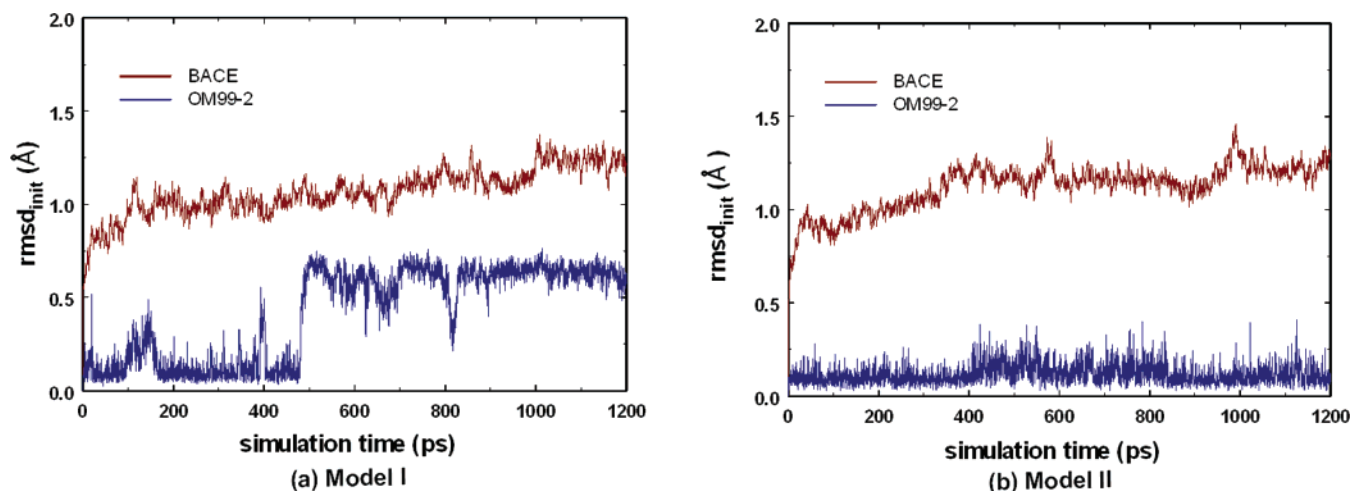


Figure 5. Comparative view of time evolutions of the root-mean-square deviations for C α atoms of BACE (red) and heavy atoms of OM99-2 (blue) in (a) Model I and (b) Model II.

for OM99-2 within the active site might explain why the structure of the eight-residue inhibitor including the turn of backbone at P $_2'$ could be clearly visible in the X-ray crystal structure.^{3b} At this point, however, it is impossible to unambiguously assign the preferred protonation state of catalytic Asp diad, although a little difference in protein flexibility and ligand motion is found between Models I and II.

Due to the presence of two strong hydrogen bonds between the inhibitor hydroxyl group and the catalytic Asp diad in the original X-ray crystal structure with associated donor–acceptor distances of 2.5–2.6 Å, the determination of the protonation state of the Asp residues may be guided by comparing the dynamic properties of the two hydrogen bonds in Models I and II. Figure 6 displays the time dependence of the interatomic distances associated with the hydrogen bonds of interest. When Asp32 is neutral and Asp228 is ionized, both hydrogen bonds established between Asp32 HD2 atom and hydroxyl oxygen of OM99-2, and between Asp228 OD2 atom and the inhibitor hydroxyl hydrogen are retained for 99% of simulation time (Figure 6a). We are assuming the distance limit of O \cdots H hydrogen bond to be 2.2 Å as suggested by Jeffrey.²¹ The time average of Asp32 OD2 \cdots OM99-2 O and Asp228 OD2 \cdots OM99-2 O distances are found to be 2.78 and 2.75 Å, respectively, in a reasonable agreement with the corresponding X-ray data (Figure 6b). When the protonation states of Asp32 and Asp228 are reversed, however, the HD2 atom of Asp228 is more than 2.2 Å distant from the inhibitor hydroxyl oxygen at most of simulation time although the Asp32 seems to maintain a stable hydrogen bond with the inhibitor (Figure 6c). A consistent trend is also observed in the dynamic behaviors of the associated O \cdots O distances (Figure 6d). Judging from the difference in dynamic stability of the Asp228 \cdots OM99-2 hydrogen bond between Models I and II, it is apparent that the neutral form of Asp228 would be inadequate for stabilizing the inhibitor hydroxyl group, providing an evidence for the protonation state with neutral Asp32 and ionized Asp228.

To check the possibility of the formation of a new stable hydrogen bond between Asp228 and the inhibitor hydroxyl moiety due to the rotation of the carboxylic acid group in Model

II, we have examined the time dependence of the distance between OD1 atom of Asp228 and the inhibitor hydroxyl group, which is shown in Figure 7. Although the OD1 atom stays in proximity of the hydroxyl oxygen of OM99-2, the O \cdots H distance is larger than 2.2 Å for 96% of the simulation time, disproving the formation of a stable hydrogen bond. These results indicate that the OD1 atom should accept a hydrogen bond from other enzymatic group.

In Figure 8 the representative MD trajectory snapshots for the two model systems under consideration are compared. In Model I, the sidechains of Ser35 and Thr231 reside in close proximity to the catalytic Asp diad, as in the X-ray crystal structure of BACE-OM99-2 complex, donating a hydrogen bond to Asp32 and Asp228, respectively. Most probably, these hydrogen bonds would be responsible for positioning Asp32 and Asp228 to interact with the inhibitor hydroxyl group in a stable manner. When the protonation states of Asp32 and Asp228 are reversed, however, both Ser35 \cdots Asp32 and Thr231 \cdots Asp228 hydrogen bonds are ruptured with the protonated OD2 atom of Asp228 moving from the inhibitor hydroxyl group to Asp32, leading to the formation of a new hydrogen bond. In this structure, the role of hydrogen bond acceptor for the OG1 atom of Thr231 is played by the unprotonated OD1 atom of Asp228.

The roles of Ser35 and Thr231 in stabilizing the hydrogen bonds between the catalytic Asp diad and the inhibitor hydroxyl moiety can be manifested by examining the dynamic properties of their respective interactions with Asp32 and Asp228. Figure 9a illustrates the time dependence of the two hydrogen bonds of interest in Model I. As expected, both Ser35 \cdots Asp32 and Thr231 \cdots Asp228 hydrogen bonds are maintained throughout most of the simulation time, although the former becomes unstable from time to time. The hydrogen bond distance of the latter remains shorter than that of the former for 82% of the simulation time, suggesting that the role of Thr231 would be more significant than that of Ser35 in stabilizing the hydrogen bonds between the catalytic Asp diad and the inhibitor hydroxyl group. In contrast to the results for Model I, both of the two hydrogen bonds in Model II are ruptured at an early stage of simulation (Figure 9b). Although the Ser35 \cdots Asp32 hydrogen bond lasts for about 30 ps, the Thr231 \cdots Asp228 hydrogen bond

(21) Jeffrey, G. A. *An Introduction to Hydrogen Bonding*; Oxford University Press: Oxford, 1997.

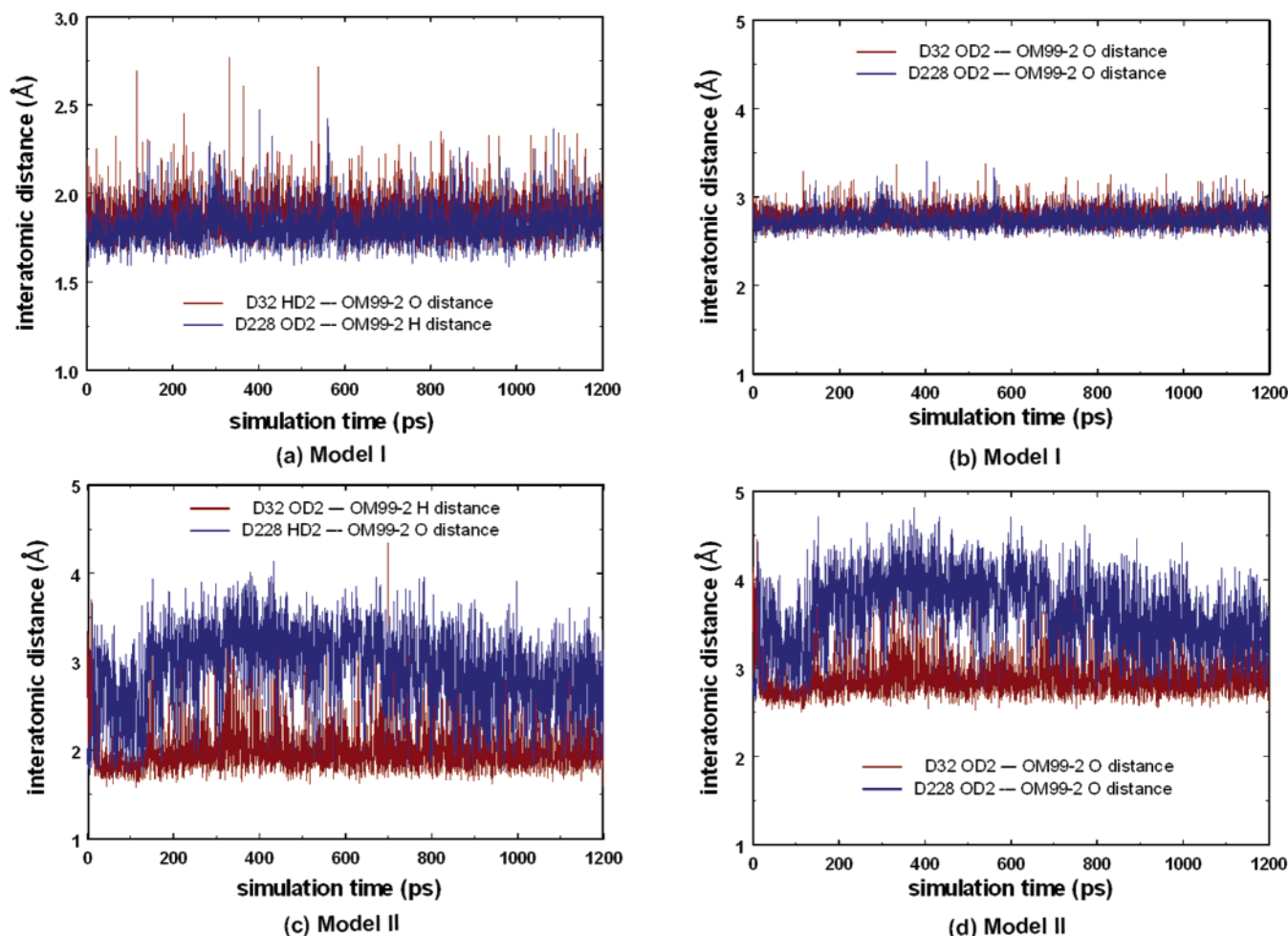


Figure 6. (a) Time evolution of the distances between HD2 atom of Asp32 and hydroxyl oxygen of OM99-2 (red), and between OD2 atom of Asp228 and hydroxyl hydrogen of OM99-2 (blue) in Model I. (b) Time evolution of the distances between OD2 atom of Asp32 and hydroxyl hydrogen of OM99-2 (red), and between HD2 atom of Asp228 and hydroxyl oxygen of OM99-2 (blue) in Model II.

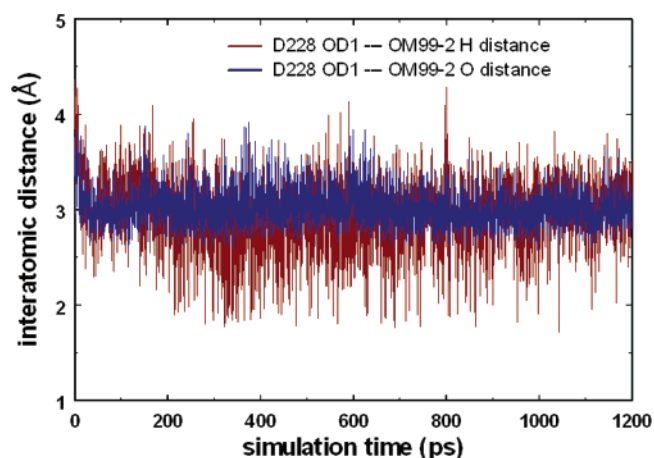


Figure 7. Time dependence of the interatomic distances between OD1 atom of Asp228 and the hydroxyl group of the inhibitor OM99-2 in Model II.

breaks in a few picoseconds of production dynamics, indicating that its breakage would initiate the rupture of the whole hydrogen bond network that are established in the form of Ser35...Asp32...OM99-2...Asp228...Thr231.

The rupture of the Thr231...Asp228 hydrogen bond in Model II leads to the change of the hydrogen acceptor for Asp228 from

the inhibitor hydroxyl group to the side chain carboxylate group of Asp32. As can be seen in Figure 10, the hydrogen bond between Asp32 OD2 atom and Asp228 HD2 atom is observed first at 15 ps and stabilized at around 180 ps, indicating that its formation lags behind the breakage of the Thr231...Asp228 hydrogen bond. The time lag of 165 ps seems to be required for the protein conformation to be adjusted to the local change in the hydrogen-bonding network.

To get further evidence for the preferred protonation state, we carried out docking experiment of the novel potent inhibitor WO02088101 in the active site of BACE with varying protonation states of the catalytic Asp diad. The DOCK program is used in this comparative analysis because it has been shown to be a promising tool for the identification of macromolecule ligands.²² As might be expected, the binding energy of the ligand in Model I is about 3 kcal/mol larger than that in Model II (Figure 11). The reported K_i value of WO02088101 is less than 3 nM. Obviously, the protonation state in Model I is more consistent with such a high inhibitory activity.

(22) (a) Kuntz, I. D.; Meng, E. C.; Shoichet, B. K. *Acc. Chem. Res.* **1994**, *27*, 117–123. (b) Filikov, A. V.; James, T. L. *J. Comput.-Aided Mol. Des.* **1998**, *12*, 229–240. (c) Shoichet, B. K.; Stroud, R. M.; Santi, D. V.; Kuntz, I. D.; Perry, K. M. *Science* **1993**, *259*, 1445–1450. (d) Bodian, D. L.; Yamasaki, R. B.; Buswell, R. L.; Stearns, J. F.; White, J. M.; Kuntz, I. D. *Biochemistry* **1993**, *32*, 2967–2978. (e) Ring, C. S.; Sun, E.; McKerrow, J. H.; Lee, G. K.; Rosenthal, P. J.; Kuntz, I. D.; Cohen, F. E. *Proc. Natl. Acad. Sci.* **1993**, *90*, 3583–3587.

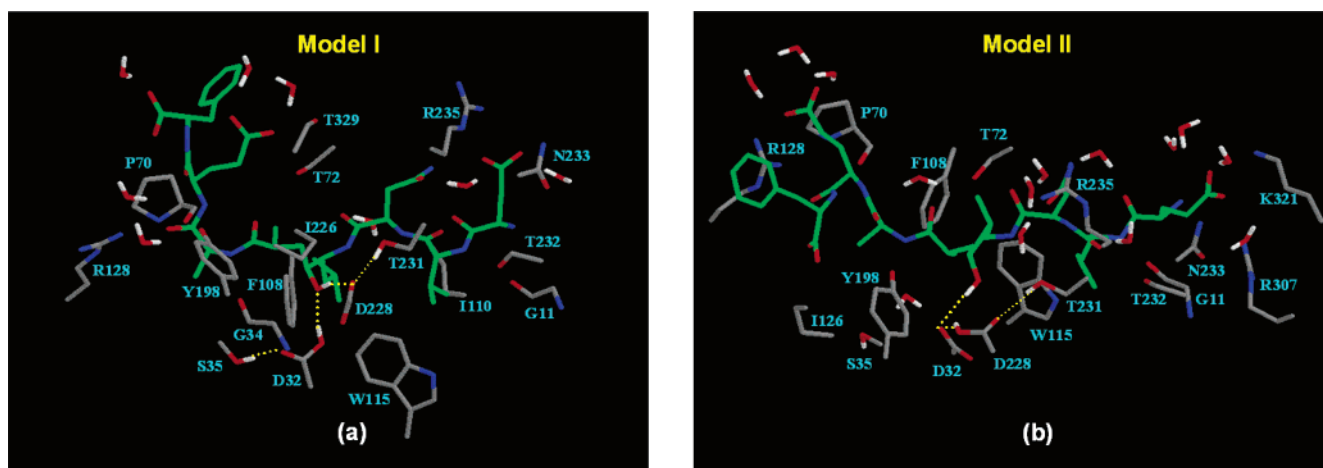


Figure 8. Comparative view of the representative MD trajectory snapshots in (a) Model I and (b) Model II. Yellow dotted line indicate hydrogen bonds. Solvent water molecules found near the inhibitor-binding site are also shown.

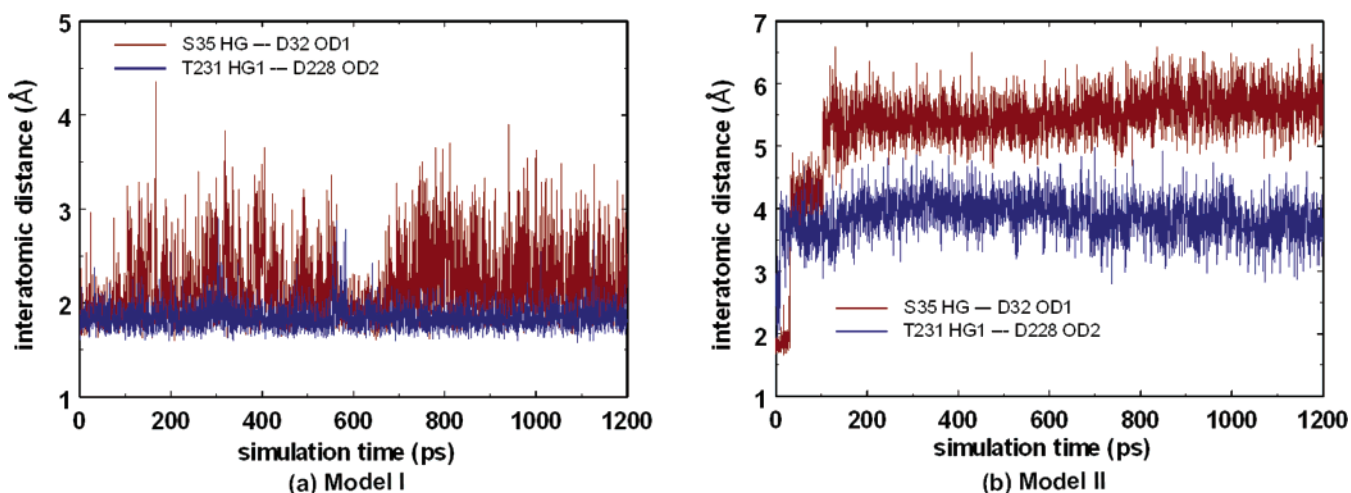


Figure 9. Time evolution of the distances between Ser35 HG atom and Asp32 OD1 atom (red), and between Thr231 HG1 atom and Asp228 OD2 atom (blue) in (a) Model I and (b) Model II.

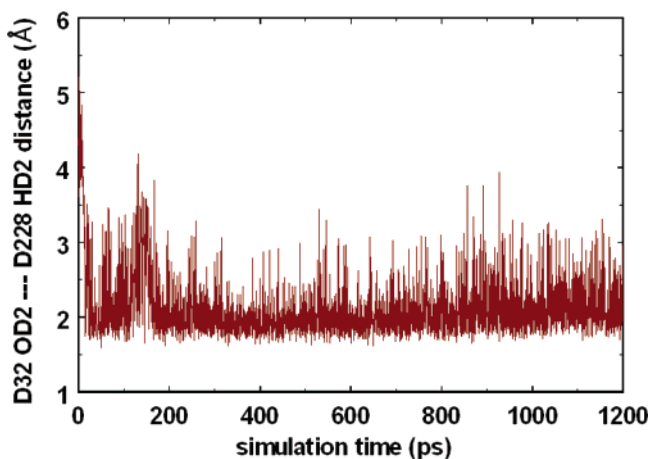


Figure 10. Maintenance of the hydrogen bond between Asp32 and Asp228 during the entire course of simulation in Model II.

Another important aspect is that the ligand adopts two different binding modes in accordance with the protonation states of the catalytic diad in BACE active site. Although the overall conformation of the inhibitor remains very similar in the two binding modes, the docked orientation of the inhibitor is rotated by 180° with respect to an axis connecting the two

phenyl and the piperazine rings with the change of the protonation states of Asp32 and Asp228. In addition, the inhibitor piperazine moiety forms a hydrogen bond with Asp228 in one binding mode (Figure 11a), whereas it is located more than 5 \AA away from both catalytic Asp residues and donates a hydrogen bond to the backbone carbonyl oxygen of Thr231 in the other binding mode (Figure 11b). Because the binding of an inhibitor group to the catalytic Asp diad is believed to be a key feature in the inhibition of BACE activity, such a difference in docked structure of the inhibitor WO02088101 can be taken as an additional support for the protonation state involving neutral Asp32 and ionized Asp228.

Hence, the characteristic that discriminates the neutral Asp228 from its ionized form should be the inability to form a stable hydrogen bond with hydroxyl and piperazine group of the inhibitors. Basically, such a difference stems from the decrease in basicity of the carboxylate oxygen due to the protonation, which is related to the difference in atomic charges between the two protonation states. Indeed, the RESP and Gasteiger–Marsili charges of OD2 atom of the neutral Asp residue become 0.164 and 0.219 e less negative upon protonation, respectively. Therefore, the disappearance of the hydrogen bond between Asp228 and the inhibitor groups in Model II can be attributed to the decrease in electrostatic interaction, which is known to

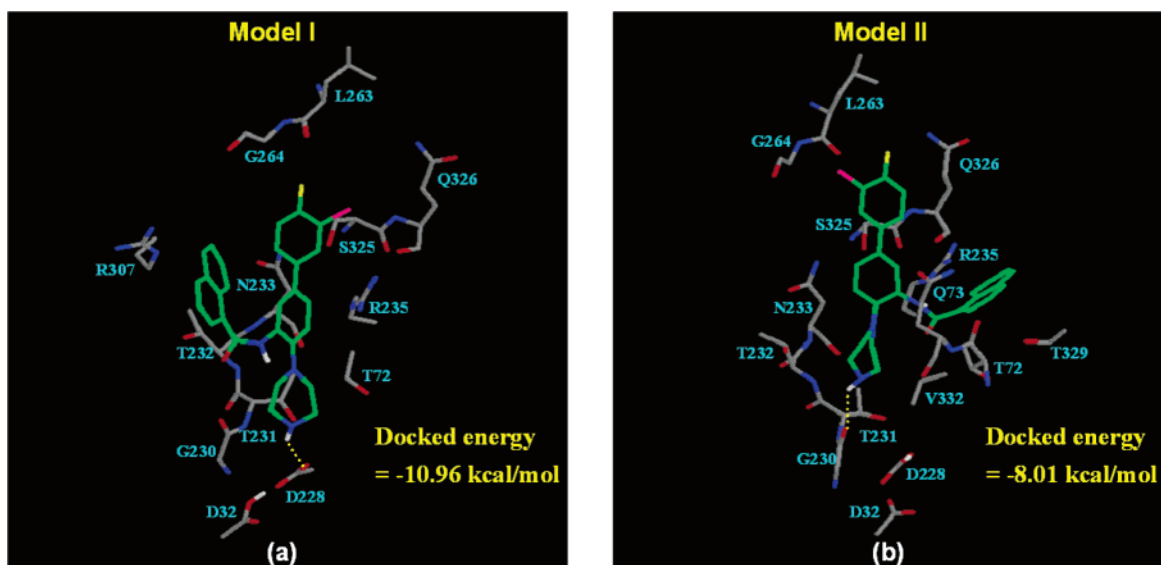


Figure 11. Comparative view of the docked structures of the inhibitor WO02088101 in the BACE active site with the protonation states in (a) Model I and (b) Model II.

be the most significant energy ingredient of a hydrogen-bond complex.²³

Conclusions

From MD simulation studies of β -secretase complexed with the inhibitor OM99-2, we have found that only the protonation state of catalytic Asp diad with neutral Asp32 and ionized Asp228 can explain the structural features of their interactions with the inhibitor hydroxyl group found in the previous X-ray crystallographic analyses. In this protonation state, a series of hydrogen bonds established in the form of Ser35 \cdots Asp32 \cdots OM99-2 \cdots Asp228 \cdots Thr231 is maintained throughout most of the simulation time. When Asp228 is in the neutral form, on the other hand, it is incapable of forming a hydrogen bond with the inhibitor, due to its higher affinity for the carboxylate side

chains of Asp32. As a result, the Ser35 \cdots Asp32 hydrogen bond is also broken. These undesirable structural changes should be attributed to the rupture of the Asp228 \cdots Thr231 hydrogen bond because it occurs at the earliest stage of simulation. Hence, the results of MD simulations suggest that neutral Asp32 and ionized Asp228 are adequately positioned by Ser35 of Thr23, respectively, in enzymatic catalysis and inhibitor binding. The energetic and structural features found in docking experiments also support the protonation state with neutral Asp32 and ionized Asp228. In this state, the novel potent inhibitor WO02088101 is found to be more stabilized than in the alternative protonation state by 3 kcal/mol, allowing the piperazine moiety to form a direct hydrogen bond with the Asp228.

Acknowledgment. This work was supported by a grant from the Center for Molecular Catalysis of the Korea Science and Engineering Foundation.

(23) (a) Umeyama, H.; Morokuma, K. *J. Am. Chem. Soc.* **1977**, *99*, 1316–1332. (b) Chen, W.; Gordon, M. S. *J. Phys. Chem.* **1996**, *100*, 14 316–14 328. (c) Park, H.; Lee, H. *Chem. Phys. Lett.* **1999**, *301*, 487–492.

JA0304493